Phenomenological approach to transport through three-terminal disordered wires

A. M. Martínez-Argüello,[1,2,*] J. A. Méndez-Bermúdez,[2,†] and M. Martínez-Mares[3,‡]

[1]*Instituto de Ciencias Físicas, Universidad Nacional Autónoma de México, Apartado Postal 48-3, 62210, Cuernavaca Mor., Mexico*

[2]*Instituto de Física, Benemérita Universidad Autónoma de Puebla, Apartado Postal J-48, 72570 Puebla, Mexico*

[3]*Departamento de Física, Universidad Autónoma Metropolitana-Iztapalapa, Apartado Postal 55-534, 09340 Ciudad de México, Mexico*

(Received 15 November 2018; published 4 June 2019)

We study the voltage drop along three-terminal disordered wires in all transport regimes, from the ballistic to the localized regime. This is performed by measuring the voltage drop on one side of a one-dimensional disordered wire in a three-terminal setup as a function of disorder. Two models of disorder in the wire are considered: (i) the one-dimensional Anderson model with diagonal disorder and (ii) finite-width bulk-disordered waveguides. Based on the known β dependence of the voltage drop distribution of the three-terminal chaotic case, β being the Dyson symmetry index ($\beta = 1$, 2, and 4 for orthogonal, unitary, and symplectic symmetries, respectively), the analysis is extended to a continuous parameter $\beta > 0$ and uses the corresponding expression as a phenomenological one to reach the disordered phase. We show that our proposal encompasses all the transport regimes with β depending linearly on the disorder strength.

DOI: 10.1103/PhysRevE.99.062202

I. INTRODUCTION

Quantum transport through mesoscopic systems and nanostructures with complex dynamics has been of great interest for a long time (see, for instance, Refs. [1–3] and references therein). The earlier experiments considered conductors of normal metal whose size is larger than the elastic mean free path. Quantum coherence along the sample with randomly distributed impurities gives rise to striking quantum interference effects, as well as to sample-to-sample fluctuations in the transport properties, due to the different microscopic configurations of disorder, that were the subject of intense research [4–7]. These transport properties and fluctuations have been proven to be very well described by means of a diffusion equation, in a Fokker-Planck form, known as the Dorokhov-Mello-Pereyra-Kumar (DMPK) equation [8–10] and by the equivalent supersymmetric nonlinear σ model [11–13]. It is in this framework where the study of universal conductance fluctuations (UCF) [14–16], weak localization [10], and the metal-insulator transition [17,18] have been successfully addressed, all of them in two-probe configurations (see also Ref. [1] and the references therein). However, to allow for a quantitative comparison with experiments, multiprobe approaches have been of great importance [19–26] since most of the experiments in nanoestructures are performed in multiterminal arrangements [27–30]. Furthermore, striking effects due to backscattering [31,32], of geometrical nature, as well as the need to take into account the actual measuring geometry in those configurations have been pointed out [20]. More recently, the statistical fluctuations of the transport properties through clean quantum devices with chaotic classical dynamics have been investigated [1,2,33,34].

Of particular interest are three-terminal systems since they offer potential applications [35,36]; for instance, three-terminal systems are used to sense the coupling strength between individual leads and the different modes in the device to which they are coupled [37]. The fluctuations of the voltage drop along an electronic device was first studied in disordered wires [21,38], while in chaotic devices was considered in Ref. [39], using random matrix theory simulations. Furthermore, for the particular three-terminal configuration, where the voltage probe is on one side of the chaotic wire, an analytical expression for all symmetry classes (orthogonal, unitary, and symplectic), as well as an auxiliary experiment with chaotic microwave graphs that verifies the theoretical prediction, were presented in Ref. [40].

In this paper we study the voltage drop on one side of disordered wires for all transport regimes. The system is studied by the scattering matrix approach and, in order to validate our results, we appeal to two models to describe the disordered wire: the finite size one-dimensional Anderson model (AM) with diagonal disorder and finite-width bulk-disordered (BD) waveguides. Our analysis is based on the distribution of the voltage drop, whose dependence on the Dyson parameter β is explicit ($\beta = 1$ for the orthogonal symmetry, $\beta = 2$ for the unitary one, and $\beta = 4$ for the symplectic symmetry). This distribution is extended to continuous β, which is used as a phenomenological expression. We show that this procedure describes all transport regimes, deep from the ballistic to the localized regime, where the Dyson parameter β may be interpreted as the degree of disorder since it depends only on the ratio between the localization length and the system size. Our results are in agreement with numerical simulations and may be verified experimentally in single-mode waveguides with either bulk or surface disorder.

*blitzkriegheinkel@gmail.com

†jmendez@ifuap.buap.mx

‡moi@xanum.uam.mx

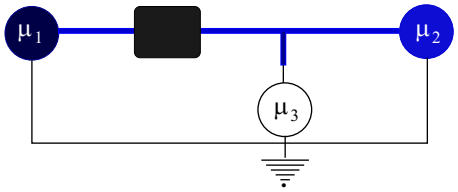

FIG. 1. Sketch of a three-probe setting that allows the measurement of the voltage drop along a device, represented by the horizontal wire. A flux current is established along the horizontal wire, while the vertical wire measures the voltage drop μ_3, which depends on the chemical potentials μ_1 and μ_2. The thick (blue) lines represent perfect conductors connected to the sources of voltages.

The paper is organized as follows. In Sec. II we summarize the main results about the voltage drop in three-terminal devices when the voltage probe is on one side of a disordered wire. Also, there, we present the corresponding statistical distribution and emphasize the Dyson parameter dependence when the wire is a chaotic cavity. In Sec. III we present the description of the disordered wire in terms of the open one-dimensional Anderson model, while a finite-width bulk-disordered waveguide realization is presented in Sec. IV. We present our conclusions in Sec. V.

II. VOLTAGE DROP IN A THREE-TERMINAL DEVICE

In the Landauer-Büttiker formalism of multiterminal devices the electronic transport is reduced to a scattering problem [19]. The simplest arrangement that allows the measurement of the voltage drop along a device is a three-probe setting. As an example we consider the system shown in Fig. 1 in which the device, represented by the black box, is connected via perfect leads (thick blue lines) to fixed sources of voltages $\mu_1(= eV_1)$ and $\mu_2(= eV_2)$ that induce a flux current along the wire. The voltage drop can be measured by means of a third wire (vertical thick blue line) used as a probe. This can be achieved by fulfilling the requirement that the current passing through the probe vanishes, thus yielding to the voltage drop $\mu_3(= eV_3)$ along the device, namely [20]

$$\mu_3 = \frac{1}{2}(\mu_1 + \mu_2) + \frac{1}{2}(\mu_1 - \mu_2)\, f, \tag{1}$$

with

$$f = \frac{T_{31} - T_{32}}{T_{31} + T_{32}}, \tag{2}$$

where T_{31} and T_{32} are the transmission probabilities from wire 1 to wire 3 and from wire 2 to wire 3, respectively.

Since the electrons travel freely through each perfect lead and suffer a scattering process due to the disordered wire, the quantity f depends on the intrinsic nature of the conductor and contains all the relevant information about the multiple scattering in the device. If the device is a disordered or a chaotic wire, f fluctuates in the interval $[-1, 1]$ since μ_3 cannot reach either the value μ_1 or μ_2 due to the contact resistance [20].

Since the most interesting effects of quantum interference occur for a few number of transmitting modes, we concentrate our attention to the situation in which the perfect leads are single-mode waveguides and that the probe is symmetrically coupled to the other two terminals at the junction. In that case the scattering matrix that describes the wire is a 2×2 matrix which has the general form

$$S = \begin{pmatrix} r & t' \\ t & r' \end{pmatrix}, \tag{3}$$

where r (r') and t (t') are the reflection and transmission amplitudes when incidence is from the left (right) of the wire, and Eq. (2) takes the form [40]

$$f = \frac{|t|^2 - |1 - r'|^2}{|t|^2 + |1 - r'|^2}. \tag{4}$$

Chaotic wire

For the case in which the wire is a chaotic cavity, S is chosen from an appropriate ensemble of scattering matrices according to the symmetry present in the system. That is, S belongs to one of the so-called circular ensembles from random matrix theory, with β representing the symmetry class present in the system: in the absence of any symmetry, flux conservation condition is the only requirement S must fulfill, it becomes a unitary matrix, $SS^\dagger = \mathbb{1}$ with $\mathbb{1}$ the 2×2 unit matrix, and S belongs to the circular unitary ensemble (CUE). The presence of time reversal symmetry defines the circular orthogonal ensemble (COE), in which case S is a symmetric unitary matrix, $S = S^T$, where T stands for the transpose. Finally, the presence of time reversal and spin-rotation symmetries define the circular symplectic ensemble (CSE), in which S is a self-dual quaternion matrix and satisfies $S^{\mathrm{R}} = S$ and the flux conservation condition reads $SS^* = \mathbb{1}$, where S^* is the complex quaternion of S. In the Dyson scheme, these ensembles are labeled by $\beta = 1$, 2, and 4, respectively [41]. For these symmetry classes, the statistical distribution of f is given by [40]

$$p_\beta(f) = \begin{cases} \frac{1}{\pi}\sqrt{(1-f)/(1+f)} & \text{for } \beta = 1, \\ \frac{1}{2}(1-f) & \text{for } \beta = 2, \\ \frac{3}{4}(1+f)(1-f)^2 & \text{for } \beta = 4, \end{cases} \tag{5}$$

which can be written in a single equation as

$$p_\beta(f) = 2^{1-\beta}\frac{\Gamma(\beta)}{[\Gamma(\beta/2)]^2}\frac{(1-f)^{\beta/2}}{(1+f)^{1-\beta/2}}. \tag{6}$$

This distribution is the main quantity on which this paper is focused. It is obtained under very general random-matrix and maximum-entropy considerations implied by the invariant measure of scattering matrices. At its core it has a Coulomb gas interpretation for the transmission eigenvalues distribution, corresponding to the distribution of the eigenvalues, τ_n, of the Hermitian matrix $tt^\dagger$ of random scattering matrices, which for $\tau_n = 1/(1 + \lambda_n)$ yields to a Coulomb gas form for the parameters λ_n. It was first proposed by Dyson and Wigner in the study of energy eigenvalues of ensembles of random Hermitian matrices in which β depends inversely on the temperature and can take on any positive value [41,42]. Thus, in our study, we first relax β to be real positive while preserving the conservation of total probability of $p_\beta(f)$ of Eq. (6), and then it is proposed as a phenomenological expression. We show that it covers all transport regimes, from the ballistic to

the deep localized regime. To verify the validity of our assertion we make use of two models for the description of the disorder in the wire: the open one-dimensional Anderson model (AM) and finite-width bulk-disordered (BD) waveguides. This approach has been used, for instance, in the study of the level spacing distribution and verified in several physical systems: the kicked rotator [43], the Dyson's Coulomb gas [44], and recently in the one-dimensional Anderson model, where the continuous $\beta > 0$ has been interpreted as degree of disorder or internal chaos [45]. Therefore, we should stress that the parameter β in the distribution of Eq. (6) is here interpreted as degree of disorder and does not have to be related to the Dyson symmetry index.

III. OPEN 1D ANDERSON MODEL: EFFECTIVE HAMILTONIAN APPROACH

A model of disorder in the wire can be implemented in an N-site one-dimensional wire of length L described by the tight-binding Hamiltonian H with nearest neighbor interactions of the form

$$H_{mn} = \varepsilon_n \delta_{mn} - v(\delta_{m,n+1} + \delta_{m,n-1}), \tag{7}$$

where ε_n is the energy of site n, v is the tunnel transition amplitude to nearest neighbor sites, and δ is the usual Kronecker delta. For diagonal disorder v is just a constant, that we fix to $v = 1$, while the site energy ε_n is a random number which for simplicity we consider uniformly distributed in the interval $[-w/2, w/2]$ with variance $\sigma^2 = \langle \varepsilon_n^2 \rangle = w^2/12$, and w being a measure of the amount of disorder.

We open the wire by attaching it on the left ($L = 1$) and right ($L = N$) ends to semi-infinite single-mode perfect leads with coupling strength $\gamma^{\mathrm{L,R}}$ to the left (L) and to the right (R) end, respectively. The 2×2 S matrix can be written in the form [28]

$$S(E) = \mathbb{1} - 2i \sin(k) W^T \frac{1}{E - \mathcal{H}_{\mathrm{eff}}} W, \tag{8}$$

where E is the energy, $k = \arccos(E/2)$ is the wave vector supported in the leads, and $\mathcal{H}_{\mathrm{eff}}$ is the effective non-Hermitian Hamiltonian, namely

$$\mathcal{H}_{\mathrm{eff}} = H - \frac{e^{ik}}{2} W W^T. \tag{9}$$

In Eqs. (8) and (9) the matrix $W(E)$ describes the coupling of the wire with the leads. Its elements are defined by

$$W_{mn} = 2\pi \sum_{c=\mathrm{L,R}} A_m^c(E) A_n^c(E), \tag{10}$$

with the coupling amplitudes

$$A_n^{\mathrm{L,R}}(E) = \sqrt{\frac{\gamma^{\mathrm{L,R}}}{\pi}} \left(1 - \frac{E^2}{4}\right)^{1/4} \left(\delta_{n,1}^{\mathrm{L}} + \delta_{n,N}^{\mathrm{R}}\right). \tag{11}$$

Furthermore, the energy dependence in $\mathcal{H}_{\mathrm{eff}}$ can be neglected since $\arccos(E/2)$ changes slightly at the center of the band. Moreover, the inverse localization length reduces to $\ell_\infty^{-1}(E) = w^2/105.2$ [46], which means that the higher the intensity of disorder the smaller the localization length is, as expected.

From Eq. (8) we observe that the reflection and transmission amplitudes t and r', respectively, that appear in the expression of f, Eq. (4), depend on the localization length and the degree of disorder. This dependence is only through the ratio $x = \ell_\infty/L$, from which x^{-1} (the length of wire in units of the localization length) can be considered as the disorder strength, satisfying a single-parameter scaling hypothesis [47]. This is verified in Fig. 2 for the distribution of (a) T_{31} and (b) T_{32}, for different wire lengths.

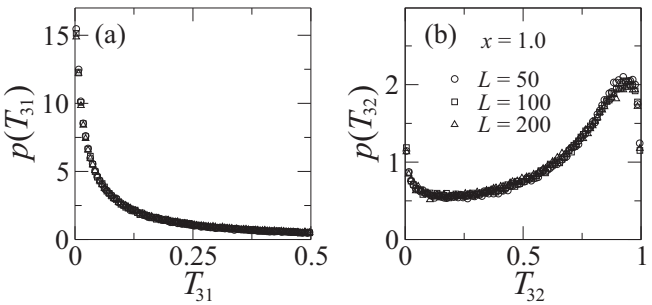

FIG. 2. Distribution of (a) T_{31} and (b) T_{32} for a fixed $x = \ell_\infty/L$ and different wire lengths, as indicated in the panels. For the numerical calculation we used an ensemble of 2×10^5 wire realizations and 100 bins to construct the histograms.

In Fig. 3 we show the behavior of distribution $p_\beta(f)$ for several values of β for (a) the analytical expression, Eq. (6), and (b) numerical simulations of f with r' and t obtained from Eq. (8). For the simulations we constructed ensembles of 2×10^5 disordered wires and used 100 bins to construct the histograms. The cases $\beta \approx 1$, 2, and 4, indicated as thick lines in panels (a) and (b), correspond roughly to the chaotic cases in the presence and absence of time-reversal invariance, and in the presence of symplectic symmetry, in continuous (black), dashed (red), and dashed-dotted (blue) lines, respectively (see Ref. [40]). They are shown for comparison purposes only. In the present case we should recall that β is a function of the strength of disorder and does not have to be confused with the Dyson symmetry index. A similar result with β very close to 1, 2, and 4 has also been obtained in the comparison

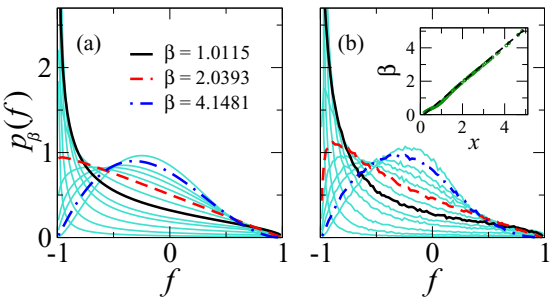

FIG. 3. Behavior of $p_\beta(f)$ for several values of β for (a) the analytical expression, Eq. (6), and (b) for numerical simulations of Eq. (8) with disorder modeled by the 1D Anderson Hamiltonian. The $\beta \approx 1$, 2, and 4 cases, indicated as thick lines in panels (a) and (b), correspond to the chaotic cases in the presence and absence of time-reversal invariance, and in the presence of symplectic symmetry, in continuous (black), dashed (red), and dashed-dotted (blue) lines, respectively. In the inset of panel (b) we show the relationship between x and β obtained by fitting $p_\beta(f)$ to the numerical distributions (see the text).

of the phenomenological level spacing distribution function proposed by Izrailev to the Dyson's Coulomb gas [44]. Furthermore, also a continuous β has been obtained from the generalization of the DMPK equation to higher dimensions [48,49], and verified in Ref. [50], and it has also been used as a continuous parameter for the description of the conductance distribution of surface disordered waveguides [17].

The fitting between the analytical expression $p_\beta(f)$ to the numerical distribution, for each value of the ratio x, determines the corresponding value of β. For the fitting we chose x in the interval [1.7, 3.7] in order to avoid divergencies for values of f close to -1 and 1. We numerically found that the parameters x and β are related through a quadratic equation given by

$$\beta(x) \approx -4.449 \times 10^{-3}\, x^2 + 1.071\, x - 0.1806, \qquad (12)$$

with a statistical indicator of $\chi^2 = 4.34 \times 10^{-4}$, as shown in the inset of Fig. 3(b). It is worth mentioning that a linear dependence between β and x has been reported in the literature [44,51,52], as well as a nonlinear dependence [53]; here, however, a slight deviation from linearity is obtained which might be due to the invasiveness of the probe that also affects the behavior of other physical quantities. Furthermore, in Fig. 3 we observe some deviations between both distributions which are model dependent; however, the phenomenology showed by the expression of Eq. (6) is well reproduced. A continuous transition between different values of β is also observed.

In what follows we verify our proposal with a more realistic model of disorder, i.e., with finite-width BD waveguides.

IV. APPLICATION TO BULK-DISORDERED WAVEGUIDES

We validate the applicability of our proposal, Eq. (6), by means of finite element simulations of bulk-disordered waveguides. A BD waveguide consists of a quasi-one-dimensional wire formed by attaching N two-dimensional building blocks (BB). Every building block is a square cavity of side d connected to two semi-infinite leads of width d on the left and right sides. We place at random a circular obstacle of radius ρ inside each building block to produce an ensemble. The leads support plane waves with energy E; when E lies inside the interval $(\hbar^2/2md^2)[\mu^2\pi^2,\ (\mu+1)^2\pi^2]$ they support μ open channels. We use the dimensionless units $\hbar^2/2md^2 = 1$, so that one open channel (i.e., the case we will focus on below) occurs for $E \in [\pi^2, (2\pi)^2]$. We fix the energy to $E = (1.5\pi)^2$, so that both leads support one open channel and the energy is far from the new channel threshold in order to avoid threshold singularities; we also set $d = 100\rho_0$ with $\rho_0 = 1$.

To compute the scattering quantities of the bulk-disordered waveguides we use the combination rule of scattering and transfer matrices, as shown in Ref. [54]. First, by means of standard finite element methods (see, for instance, Refs. [55–57]) we compute the scattering matrix of an ith building block:

$$S^{(i)}_{\rm BB} = \begin{pmatrix} r_i & t_i' \\ t_i & r_i' \end{pmatrix}, \qquad (13)$$

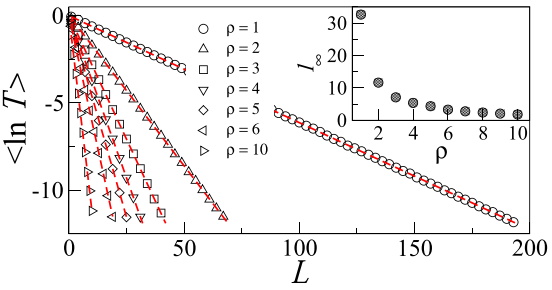

FIG. 4. Average logarithm of the conductance $\langle \ln T \rangle$ as a function of the waveguide length L for bulk-disordered waveguides (supporting one open channel) characterized by $\rho = [1, 10]$. Red-dashed lines are fittings to the data with Eq. (17); these fittings are performed to extract the localization lengths ℓ_∞. Inset: ℓ_∞ as a function of ρ. Each point in the figure is computed by averaging over an ensemble of 10^5 waveguide realizations.

where r_i (r_i') and t_i (t_i') are the reflection and transmission amplitudes, for incidence from the left (right). Then, the transfer matrix is easily obtained from the elementary relation with the S matrix [3]; this relation leads to the transfer matrix of the building block $M^{(i)}_{BB}$. Therefore, since the building blocks are attached in series, the transfer matrix M of the complete waveguide composed by $L = N$ building blocks can be easily calculated as

$$M(L) = \prod_{i=1}^{L} M^{(i)}_{\rm BB} = \begin{pmatrix} \alpha & \xi \\ \xi^* & \alpha^* \end{pmatrix}. \qquad (14)$$

Finally, the scattering matrix of the waveguide of length L is

$$S(L) = \frac{1}{\alpha^*}\begin{pmatrix} -\xi^* & 1 \\ 1 & \xi \end{pmatrix} = \begin{pmatrix} r & t' \\ t & r' \end{pmatrix}. \qquad (15)$$

For the statistical analysis we generate an ensemble of bulk-disordered waveguides from sets of different building blocks, constructed by randomly moving the inner obstacle of radius ρ. In Fig. 4 we plot the average of $\langle \ln T \rangle$, where T is given by [19,20,58,59]

$$T(L) = \mathrm{tr}(tt^\dagger) \qquad (16)$$

as a function of the waveguide length L for bulk-disordered waveguides with $\rho = [1, 10]$. Notice that the decay of $\langle \ln T \rangle$ vs L is faster the larger the value of ρ is. Thus one can use the radius of the obstacle to tune the disorder strength in our waveguides: the larger the value of ρ the stronger the disorder strength. Furthermore, by fitting these curves to [60]

$$\langle \ln T \rangle = -\frac{2L}{\ell_\infty} = -\frac{2}{x}, \qquad (17)$$

we extract the corresponding localization length ℓ_∞; see red dashed lines in Fig. 4. In the inset of Fig. 4 we show the obtained values of ℓ_∞ as a function of ρ. They are used to design waveguides characterized by specific disorder strengths through the ratio $x = \ell_\infty/L$. We restrict our analysis to building blocks with inner obstacles with radius $\rho = 1$ to get longer waveguides (see Fig. 4), but since the lengths L of the waveguides are given as integer multiples of building blocks, not any value of x is allowed.

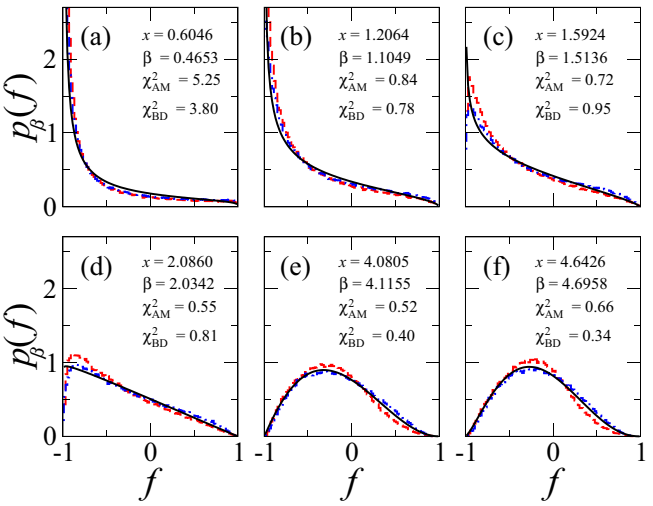

FIG. 5. Probability distribution, $p_\beta(f)$, for the three-terminal disordered device, in continuous (black) lines. The histograms correspond to the distribution of f, Eq. (4), with r' and t obtained from numerical simulations for the 1D AM (red-dashed) and for BD waveguides (blue dashed-dotted). Insets: χ^2 statistical indicator between Eq. (6) and the numerical results for both models. For the numerical analysis we performed ensembles of 2×10^5 wire realizations. For the histograms we used 100 bins.

In Fig. 5 we present probability distributions $p_\beta(f)$ for the three-terminal disordered device for different values of x, as indicated in the insets. The continuous (black) lines correspond to the analytical expression, Eq. (6), with β obtained from Eq. (12) for the corresponding x. The histograms correspond to the numerical results obtained from the two models of the disordered wire—the 1D AM of Eq. (8) (red-dashed) and for BD waveguides of Eq. (15) (blue dashed-dotted). These results show significant deviations to one another which might be due to the different nature between the models considered. On one hand, the electron diffuses away along the sample in the BD model, while, on the other hand, in the AM the electron is strongly bounded at its site and the transport takes place by hopping from one site to another. This requires a further analysis which will be addressed in a future work. However, the behavior of $p_\beta(f)$ is qualitatively captured by our expression for all the transport regimes, and it is in full agreement with the result obtained in Ref. [21] for the weak disorder case.

V. CONCLUSIONS

We studied the voltage drop along a disordered wire, in a three-terminal device. The voltage was measured by means of a third terminal, used as a voltage probe, in an asymmetric configuration; that is, when the probe is on one side of the wire. Our analysis was based on a random matrix theory result accounting for the distribution of the voltage $p_\beta(f)$, depending on a single parameter, β. For this distribution β was relaxed to take on any positive value, based on its analogy with the Coulomb gas, and proposed as a phenomenological expression covering all the transport regimes of the disordered wire, from the ballistic to the localized regime. We validate our proposal with two models for the disordered wire: the one-dimensional Anderson model and bulk-disordered waveguides. It is relevant to stress that the parameter β in $p_\beta(f)$ may be interpreted as the (reciprocal) degree of disorder in a wire of length L, and characterized by the localization length ℓ_∞, since we found that $\beta \approx \ell_\infty/L$ in a wide range of disorder strengths. Although our results show significant deviations between the numerical distributions and our proposal, which might be due to the different nature between the models considered, the phenomenology is qualitatively well captured by our proposal. A deeper analysis of the differences between these models will be addressed in a future work.

It is worth mentioning that given the wide classical wave analogies to quantum transport [61–69] our results can be tested by experiments with microwaves or mechanical waves with either surface or bulk disordered waveguides.

ACKNOWLEDGMENTS

A.M.M.-A. acknowledges Benemérita Universidad Autónoma de Puebla (BUAP), PRODEP under the Project No. DSA/103.5/16/11850, and DGAPA-UNAM for financial support. J.A.M.-B. acknowledges financial support from VIEP-BUAP (Grant No. MEBJ-EXC18-G), Fondo Institucional PIFCA (Grant No. BUAP-CA-169), and CONACyT (Grant No. CB-2013/220624). M.M.-M. acknowledges CONACyT financial support through the Grant No. CB-2016/285776.

[1] C. W. J. Beenakker, Rev. Mod. Phys. **69**, 731 (1997).
[2] Y. Alhassid, Rev. Mod. Phys. **72**, 895 (2000).
[3] P. A. Mello and N. Kumar, *Quantum Transport in Mesoscopic Systems: Complexity and Statistical Fluctuations* (Oxford University Press, New York, 2005).
[4] R. A. Webb, S. Washburn, C. P. Umbach, and R. B. Laibowitz, Phys. Rev. Lett. **54**, 2696 (1985).
[5] M. A. Paalanena, D. C. Tsui, A. C. Gossard, and J. C. M. Hwang, Solid State Commun. **50**, 841 (1984).
[6] K. Saeed, N. A. Dodoo-Amoo, L. H. Li, S. P. Khanna, E. H. Linfield, A. G. Davies, and J. E. Cunningham, Phys. Rev. B **84**, 155324 (2011).
[7] L. P. Lévy, G. Dolan, J. Dunsmuir, and H. Bouchiat, Phys. Rev. Lett. **64**, 2074 (1990).
[8] P. A. Mello, P. Pereyra, and N. Kumar, Ann. Phys. (NY) **181**, 290 (1988).
[9] P. A. Mello, Phys. Rev. Lett. **60**, 1089 (1988).
[10] P. A. Mello and A. D. Stone, Phys. Rev. B **44**, 3559 (1991).
[11] K. B. Efetov and A. I. Larkin, Zh. Eksp. Teor. Fiz. **85**, 764 (1983) [Sov. Phys. JETP **58**, 444 (1983)].
[12] K. B. Efetov, Adv. Phys. **32**, 53 (1983).
[13] A. D. Mirlin, A. Müller-Groeling, and M. R. Zirnbauer, Ann. Phys. (NY) **236**, 325 (1994).
[14] A. D. Stone, Phys. Rev. Lett. **54**, 2692 (1985).

[15] P. A. Lee and A. D. Stone, Phys. Rev. Lett. **55**, 1622 (1985).
[16] K. A. Muttalib, J.-L. Pichard, and A. D. Stone, Phys. Rev. Lett. **59**, 2475 (1987).
[17] A. García-Martín and J. J. Sáenz, Phys. Rev. Lett. **87**, 116603 (2001).
[18] L. S. Froufe-Pérez, P. García-Mochales, P. A. Serena, P. A. Mello, and J. J. Sáenz, Phys. Rev. Lett. **89**, 246403 (2002).
[19] M. Büttiker, Phys. Rev. Lett. **57**, 1761 (1986).
[20] M. Büttiker, IBM J. Res. Dev. **32**, 317 (1988).
[21] S. Godoy and P. A. Mello, Phys. Rev. B **46**, 2346 (1992).
[22] V. A. Gopar, M. Martínez, and P. A. Mello, Phys. Rev. B **50**, 2502 (1994).
[23] L. Arrachea, C. Naón, and M. Salvay, Phys. Rev. B **77**, 233105 (2008).
[24] F. Foieri, L. Arrachea, and M. J. Sánchez, Phys. Rev. B **79**, 085430 (2009).
[25] J. L. D'Amato and H. M. Pastawski, Phys. Rev. B **41**, 7411 (1990).
[26] C. J. Cattena, L. J. Fernández-Alcázar, R. A. Bustos-Marún, D. Nozaki, and H. M. Pastawski, J. Phys.: Condens. Matter **26**, 345304 (2014).
[27] A. M. Song, A. Lorke, A. Kriele, J. P. Kotthaus, W. Wegscheider, and M. Bichler, Phys. Rev. Lett. **80**, 3831 (1998).
[28] S. Datta, *Electronic Transport in Mesoscopic Systems* (Cambridge University Press, Cambridge, UK, 1995).
[29] S. Goodnick, IEEE Trans. Nanotechnol. **2**, 368 (2003).
[30] B. Gao, Y. F. Chen, M. S. Fuhrer, D. C. Glattli, and A. Bachtold, Phys. Rev. Lett. **95**, 196802 (2005).
[31] C. Texier and G. Montambaux, Phys. Rev. Lett. **92**, 186801 (2004).
[32] C. Texier and G. Montambaux, Physica E **75**, 33 (2015).
[33] C. M. Marcus, A. J. Rimberg, R. M. Westervelt, P. F. Hopkins, and A. C. Gossard, Phys. Rev. Lett. **69**, 506 (1992).
[34] P. A. Mello and H. Baranger, Interference phenomena in electronic transport through chaotic cavities: An information-theoretic approach, in *The XXXI Latin American School of Physics (Escuela Latinoamericana de Física, ELAF) New Perspectives on Quantum Mechanics*, AIP Conf. Proc. No. 464 (AIP, Melville, NY, 1999), p. 281.
[35] A. Jacobsen, I. Shorubalko, L. Maag, U. Sennhauser, and K. Ensslin, Appl. Phys. Lett. **97**, 032110 (2010).
[36] A. N. Jordan and M. Büttiker, Phys. Rev. B **77**, 075334 (2008).
[37] A. Jacobsen, P. Simonet, K. Ensslin, and T. Ihn, New J. Phys. **14**, 023052 (2012).
[38] S. Godoy and P. A. Mello, Europhys. Lett. **17**, 243 (1992).
[39] A. M. Martínez-Argüello, E. Castaño, and M. Martínez-Mares, Random matrix study for a three-terminal chaotic device, in *Special Topics on Transport Theory: Electrons, Waves, and Diffusion in Confined Systems*, AIP Conf. Proc. No. 1579 (AIP, Melville, NY, 2014), p. 46.
[40] A. M. Martínez-Argüello, A. Rehemanjiang, M. Martínez-Mares, J. A. Méndez-Bermúdez, H.-J. Stöckmann, and U. Kuhl, Phys. Rev. B **98**, 075311 (2018).
[41] F. J. Dyson, J. Math. Phys. **3**, 140 (1962).
[42] F. J. Dyson, J. Math. Phys. **3**, 157 (1962).
[43] F. M. Izrailev, Phys. Rep. **196**, 229 (1990).
[44] R. Scharf and F. M. Izrailev, J. Phys. A: Math. Gen. **23**, 963 (1990).
[45] S. Sorathia, F. M. Izrailev, V. G. Zelevinsky, and G. L. Celardo, Phys. Rev. E **86**, 011142 (2012).
[46] M. Kappus and F. Wegner, Z. Phys. B: Condens. Matter **45**, 15 (1981).
[47] P. W. Anderson, D. J. Thouless, E. Abrahams, and D. S. Fisher, Phys. Rev. B **22**, 3519 (1980).
[48] K. A. Muttalib and J. R. Klauder, Phys. Rev. Lett. **82**, 4272 (1999).
[49] K. A. Muttalib and V. A. Gopar, Phys. Rev. B **66**, 115318 (2002).
[50] P. Markoš, Phys. Rev. B **65**, 092202 (2002).
[51] G. Casati, B. V. Chirikov, I. Guarneri, and F. M. Izrailev, Phys. Rev. E **48**, R1613 (1993).
[52] J. Flores, L. Gutiérrez, R. A. Méndez-Sánchez, G. Monsivais, P. Mora, and A. Morales, Europhys. Lett. **101**, 67002 (2013).
[53] J. A. Méndez-Bermúdez, G. F. de Arruda, F. A. Rodrigues, and Y. Moreno, J. Phys. A: Math. Theor. **50**, 495205 (2017).
[54] A. Alcázar-López, J. A. Méndez-Bermúdez, and G. A. Luna-Acosta, J. Phys.: Conf. Ser. **475**, 012001 (2013).
[55] G. A. Luna-Acosta, J. A. Méndez-Bermúdez, P. Šeba, and K. N. Pichugin, Phys. Rev. E **65**, 046605 (2002).
[56] J. A. Méndez-Bermúdez, G. A. Luna-Acosta, P. Šeba, and K. N. Pichugin, Phys. Rev. E **66**, 046207 (2002).
[57] J. A. Méndez-Bermúdez, G. A. Luna-Acosta, P. Šeba, and K. N. Pichugin, Phys. Rev. B **67**, 161104(R) (2003).
[58] R. Landauer, IBM J. Res. Dev. **1**, 223 (1957).
[59] R. Landauer, IBM J. Res. Dev. **32**, 306 (1988).
[60] P. W. Anderson, Phys. Rev. **109**, 1492 (1958).
[61] E. Doron, U. Smilansky, and A. Frenkel, Phys. Rev. Lett. **65**, 3072 (1990).
[62] R. A. Méndez-Sánchez, U. Kuhl, M. Barth, C. H. Lewenkopf, and H.-J. Stöckmann, Phys. Rev. Lett. **91**, 174102 (2003).
[63] H. Schanze, H.-J. Stöckmann, M. Martínez-Mares, and C. H. Lewenkopf, Phys. Rev. E **71**, 016223 (2005).
[64] U. Kuhl, M. Martínez-Mares, R. A. Méndez-Sánchez, and H.-J. Stöckmann, Phys. Rev. Lett. **94**, 144101 (2005).
[65] S. Hemmady, X. Zheng, E. Ott, T. M. Antonsen, Jr., S. M. Anlage, Phys. Rev. Lett. **94**, 014102 (2005).
[66] D. Laurent, O. Legrand, and F. Mortessagne, Phys. Rev. E **74**, 046219 (2006).
[67] S. Bittner, B. Dietz, M. Miski-Oglu, P. O. Iriarte, A. Richter, and F. Schäfer, Phys. Rev. E **84**, 016221 (2011).
[68] A. M. Martínez-Argüello, M. Martínez-Mares, M. Cobián-Suárez, G. Báez, and R. A. Méndez-Sánchez, Europhys. Lett. **110**, 54003 (2015).
[69] E. Flores-Olmedo, A. M. Martínez-Argüello, M. Martínez-Mares, G. Báez, J. A. Franco-Villafañe, and R. A. Méndez-Sánchez, Sci. Rep. **6**, 25157 (2016).